BRIEF REPORTS AND COMMENTS

This section is intended for the publication of (1) brief reports which do not require the formal structure of regular journal articles, and (2) comments on items previously published in the journal.

Secondary ion coincidence in highly charged ion based secondary ion mass spectroscopy for process characterization

Alex V. Hamza,[a] Thomas Schenkel, Alan V. Barnes, and Dieter H. Schneider
Lawrence Livermore National Laboratory, University of California, Livermore, California 94551

(Received 2 April 1998; accepted 9 October 1998)

Coincidence counting in highly charged ion based secondary ion mass spectroscopy has been applied to the characterization of selective tungsten deposition via disilane reduction of tungsten hexafluoride on a patterned SiO_2/Si wafer. The high secondary ion yield and the secondary ion emission from a small area produced by highly charged ions make the coincidence technique very powerful. [S0734-2101(99)03601-5]

I. INTRODUCTION

In their pioneering work, Park *et al.*[1] demonstrated the use of coincidence counting in time-of-flight mass spectrometry. Time-of-flight is itself a coincidence counting technique where secondary ion stops are detected in coincidence with some start signal. In their work, Park *et al.* added an additional coincidence requirement to the time-of-flight, the requirement that a particular secondary ion be present. In order for this second coincidence requirement to provide any additional information, the secondary ion yield per primary event must be large, so that for a single primary ion event, it is possible to detect secondary ions in coincidence with the required secondary ion. In addition, the primary particles should address only a small region of the sample surface so that sample components can be spatially distinguished from one another.

Park *et al.* used ^{252}Cf fission fragments as a primary source. The fission fragments have mass in the range of 95–160 amu with kinetic energies of 60–120 MeV and charge states of 18–22+. The fission fragments excited a surface area of approximately 10–20 nm. The mass, energy and charge of the primary ions cannot be controlled in the fission fragment case. Riggi has demonstrated the coincidence counting technique for fast heavy ion primary beams[2] where the mass and velocity can be varied. In the present work, we have used a beam of slow, highly charged ions extracted from an electron beam ion trap, where the charge, energy and mass of the primary beam can be varied independently.

The interaction of slow, highly charged ions with surfaces results in the emission of a large number of secondary ions per primary ion which increases with the charge of the incident ion.[3] For example, Au^{69+} impinging on 50 nm thick SiO_2 layer on a Si wafer induces a positive secondary ion yield per primary ion of 20.[3] The surface area addressed by each highly charged ion can be estimated from the size of blister observed for single ion impacts on mica surfaces.[4] The diameter of the blisters increases from 10 to 40 nm with incident charge from 35+ to 70+. Thus, highly charged ion excitation is very well suited to coincidence time-of-flight secondary in mass spectrometry.

II. EXPERIMENT

Highly charged ions were extracted from the electron beam ion trap (EBIT) at Lawrence Livermore National Laboratory.[5] A bending magnet in the beamline between the EBIT and the ultrahigh vacuum (UHV) scattering chamber (base pressure $<3\times10^{-8}$ Pa) is used to select the mass-to-charge ratio of the incident ion beam. Time-of-flight secondary ion mass spectrometry (TOF-SIMS) was performed to measure secondary yields. The system is described in Refs. 6 and 3. Briefly, fluxes of <1000 ions per second were used and each TOF-SIMS cycle was triggered by secondary particles emitted from the target at impact of an individual highly charged ion (HCI) under normal incidence. Typical accumulation times for TOF-SIMS spectra are ~10 min. The flight path for secondary ions is ~10 cm from the surface to the annular detector. High yields of electrons and protons were used as start pulses for the time-of-flight for negative and positive secondary ions, respectively. Start efficiencies were 100% for electron starts and between 10% and 80% for proton starts. Start signals and secondary ion stop signals were detected by the same annular microchannel plate detector. The microchannel plate detection efficiency for secondary ions is estimated from the solid angle subtended and the active area to be ~10%–15%. TOF-SIMS spectra are recorded with a multistop multichannel scaler (Ortec picosecond timing analyzer, model 9308). For coincidence measurements, the events are collected in list mode, i.e., the time of

[a]Electronic mail: Hamza1@LLNL.GOV

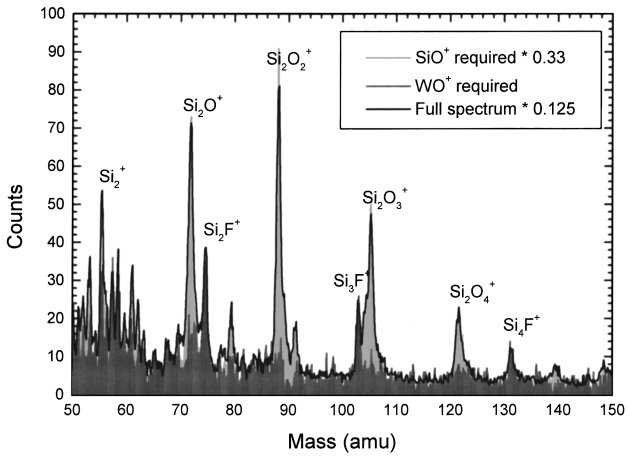

FIG. 1. Coincidence counting time-of-flight positive secondary ion mass spectrum from $W/SiO_2/Si$ test wafer with a Th^{75+} primary beam with 262.5 keV incident energy. The black line is the full spectrum divided by 8. The SiO^+ coincidence spectrum divided by 3 is shown in light gray and the WO^+ coincidence spectrum is shown in gray. The spectra are scaled based on the relative number of sweeps used to build each spectrum.

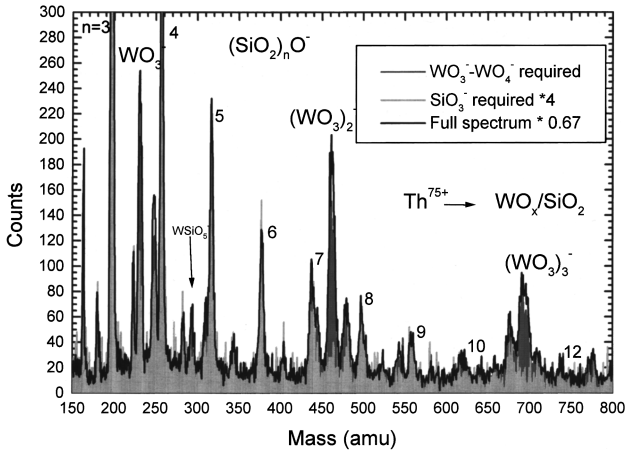

FIG. 2. Coincidence counting time-of-flight negative secondary ion mass spectrum from $W/SiO_2/Si$ test wafer with Th^{75+} primary beam at 787 keV incident energy. The black line is the full spectrum divided by 0.67. The SiO_3^- coincidence spectrum multiplied by 4 is shown in light gray and the $WO_3-WO_4^-$ coincidence spectrum is shown in gray. The spectra are scaled based on the relative number of sweeps used to build each spectrum.

each start and its associated stops are recorded in a list. The data are then filtered for particular coincidence ions. An event, a start pulse and its associated stop pulses, is accepted if the coincidence ion is present, i.e., a stop pulse is detected in a particular time window, and otherwise the event is discarded.

It takes only a few times 10^6 events to collect a spectrum. The probability of spatially overlapping ion events in the 1 mm beam spot is negligibly small. Temporal overlap contributes to the observed background. Temporally overlapping primary ion events are greatly reduced by the low flux used, 100–1000 primary ions per second. 1000 events per second corresponds to a 1%–0.5% probability of an overlapping event. Then the probability that the second primary event will produce a stop in a particular secondary ion window (100 channels/65 000 channels) is again small. Combining these two gives a small probability of counts due temporal overlap (7×10^{-6}). These are random coincidences which only dilute any observed correlations (see below).

The sample was a patterned, thermally grown SiO_2/Si test wafer that was placed in a plasma channel vapor deposition reactor for selective tungsten deposition. The SiO_2 layer is 1 μm thick. 1, 2, and 5 μm diameter via holes as well as 5–200 μm wide lines and other structures were present on the test wafer. Just prior to deposition the wafers were dipped in diluted 100:1 HF to eliminate the native oxide. Selective tungsten deposition occurred via the reaction of WF_6 with Si_2H_6 at wafer temperature of 150 °C according to the procedure reported in Ref. 7. ~150–400 nm of α-tungsten was deposited. After deposition and cooling to room temperature, the wafer was removed from the plasma reactor. The wafer was stored in air many months before being placed in the UHV scattering chamber. No *in situ* cleaning of the sample was performed.

III. RESULTS AND DISCUSSION

Figure 1 shows a portion of the positive time-of-flight secondary ion mass spectrum for a Th^{75+} primary beam with 262.5 keV kinetic energy. Summing all of the collected events gives the spectrum labeled ''full spectrum.'' Coincidence mass spectra selecting only events which have the secondary ion SiO^+ or WO^+, respectively, are also shown. The tungsten surface had become oxidized from months of storage in air; the most probably observed tungsten features were WO_x^+ secondary ions. As can be seen the Si_2O_x series is highly correlated to the SiO^+ secondary ion and the Si_xF series is highly correlated to the WO^+ secondary ion. The degree of correlation can be quantitatively determined from

$$\mathbf{C}(A^+,B^+)=P(A^+,B^+)/[P(A^+)P(B^+)], \tag{1}$$

where $P(A^+)$ is the probability of observing a given secondary ion, A^+, and $P(A^+,B^+)$ is the probability of observing B^+ in coincidence with A^+.[1] Experimentally, the probability of observing a given secondary ion is defined by the number of counts in the secondary ion peak divided by the number of primary ions striking the sample (or the number of start pulses). If **C** equals 1, the ions are independent of one another. If **C** is greater than 1, the ions are correlated; the emission of one ion tends to occur with the emission of the other. If **C** is less than 1, the ions are anticorrelated; the emission of the ion tends to preclude the emission of the other. For example, $\mathbf{C}(WO^+,Si_2F^+)=1.86$ or the Si_2F^+ secondary ion is emitted with the WO^+ secondary ion. In contrast $\mathbf{C}(SiO^+,Si_2F^+)=0.77$ or the emission of SiO^+, tends to preclude the emission of Si_2F^+. Thus, it is 2.4 times more likely that the Si_2F^+ secondary ion feature came from within 40 nm of the deposited tungsten than from within 40 nm of

the silicon dioxide area of the wafer. Similarly, the correlation of the Si_2O^+ secondary ion can be addressed. $\mathbf{C}(SiO^+,Si_2O^+)=1.98$ and $\mathbf{C}(WO^+,Si_2O^+)=0.29$; it is 6.8 times more likely that the Si_2O^+ secondary ion feature came from within 40 nm of the silicon dioxide area of the wafer than the deposited tungsten. Given that the tungsten is deposited from the reduction of WF_6 with disilane, the Si_xF secondary ion impurity series is a by-product of the reduction that deposits with the tungsten.

The coincidence counting technique shows the Si_xF impurity is localized on the deposited tungsten regions and can be assigned as a result of the WF_6 reduction step in the processing. In this example, the tungsten features were rather large (greater than or equal to a micron) and other techniques could have been applied to determine the location of the Si_xF impurity, i.e., focused ion beam secondary ion mass spectrometry or scanning Auger electron microscopy. However, as the feature sizes get smaller the number of impurity atoms or molecules analyzed in the focus area of the ion beam becomes vanishing small. The coincidence technique can analyze many similar features simultaneously, thus, removing the restrictions due the number of impurities in one small feature. In addition, the highly charged ion primary beam gives a higher ionization probability[8] and hence a higher useful yield, particularly for molecular species, for sensitive analysis of small features.

Figure 2 shows the negative time-of-flight secondary ion mass spectrum for a Th^{75+} primary beam with 787 keV kinetic energy. Summing all of the collected events gives the spectrum labeled ''full spectrum.'' Coincidence mass spectra selecting only events which have the secondary ion SiO_3^- or $WO_3-WO_4^-$, respectively, are also shown. The characteristic secondary cluster ions, $(SiO_2)_nO^-$, for a highly charged ion impinging on a silicon dioxide surface are seen out to $n=12$ for the SiO_3^- coincidence spectrum.[3,9] The $WO_3-WO_4^-$ coincidence spectrum shows a series of cluster secondary ions $(WO_3)_n^-$ out to $n=3$. The coincidence technique allows the separation of the tungsten oxide cluster series from the silicon dioxide cluster series even though the cluster ions have many overlapping peaks at the mass resolution ($m/\Delta m=200$) of a short, high transmission spectrometer.

IV. SUMMARY

Coincidence requirements in time-of-flight secondary ion mass spectrometry enhances the available information, in particular, the nanoscopic chemical heterogeneity, from the investigated surface. Slow, highly charged ions are ideally suited to coincidence counting in TOF-SIMS due the high secondary ion yield at high charge states and the small localized area interrogated by each primary ion. In this report, we have applied this technique to the analysis of the selective deposition of tungsten on patterned SiO_2/Si wafers. Impurity secondary ions were associated with the tungsten features and could be related to the processing, i.e., the reduction of WF_6 with disilane.

ACKNOWLEDGMENTS

This work was performed under the auspices of the U.S. Department of Energy at Lawrence Livermore National Laboratory under Contract No. W-7405-ENG-48.

[1]M. A. Park, K. A. Gibson, L. Quinones, and E. A. Schweikert, Science **248**, 988 (1990).
[2]F. Riggi, Nucl. Instrum. Methods Phys. Res. B **79**, 230 (1993).
[3]T. Schenkel, A. V. Barnes, M. A. Briere, A. Hamza, A. Schach von Wittenau, and D. H. Schneider, Nucl. Instrum. Methods Phys. Res. B **125**, 153 (1997).
[4]C. Rühlicke, M. A. Briere, and D. Schneider, Nucl. Instrum. Methods Phys. Res. B **99**, 528 (1995).
[5]D. Schneider, M. W. Clark, B. M. Penetrante, J. McDonald, D. DeWitt, and J. N. Bardsley, Phys. Rev. A **44**, 3119 (1991).
[6]D. Schneider and M. A. Briere, Phys. Scr. **35**, 228 (1996).
[7]T. Ohba, T. Suzuki, T. Hara, Y. Furumura, and K. Wada, in *Tungsten and Other Refractory Metals of VLSI Applications IV*, edited by R. S. Blewer and C. M. McConica (Materials Research Society, Pittsburgh, PA, 1989), pp. 17–26.
[8]T. Schenkel, A. V. Barnes, A. V. Hamza, D. H. Schneider, J. C. Banks, and B. L. Doyle, Phys. Rev. Lett. **80**, 4325 (1998).
[9]T. Schenkel, A. V. Barnes, A. V. Hamza, and D. H. Schneider, Eur. Phys. J. D **1**, 297 (1998).